



Effects of operational parameters on the photodegradation of 2,4-dinitrophenol in TiO₂ dispersion

Lu Mao, Jiaojun Shen, Xiaoliang Ma, Zhonghui Lan, Xu Zhang*

Hubei Biomass-Resource Chemistry and Environmental Biotechnology Key Laboratory, School of Resources and Environmental Science, Wuhan University, Wuhan 430079, P.R. China, Tel. +86 27 68772910; Fax: +86 27 68778893; emails: 312603022@qq.com (L. Mao), 786572688@qq.com (J. Shen), 1056149167@qq.com @126.com (X. Ma), 1354425356@qq.com (Z. Lan), xuzhangwhu@gmail.com (X. Zhang)

Received 25 October 2013; Accepted 17 June 2014

ABSTRACT

Photocatalytic degradation of 2,4-dinitrophenol in two commercial TiO₂ (Degussa P25 and Hombikat UV-100) was investigated in this work. The properties of two TiO₂ were systematically studied and described in detail. The observed photoactivity of Degussa P25 was 6–12 times higher than Hombikat UV-100 although the specific surface area of Hombikat UV-100 was 5.7 times more than that of Degussa P25. The photodegradation of 2,4-dinitrophenol was favored at neutral pH in Degussa P25, while its degradation was preferred at pH 3.0 in Hombikat UV-100 dispersion. The observed kinetic constant (k_{obs}) for the photodegradation of 2,4-dinitrophenol in 20 mg/L humic acid solution was found to be 15% (Degussa P25) and 21% (Hombikat UV-100) of the values obtained from the corresponding pure aquatic solutions. The suppression effects of β -cyclodextrin on the photodegradation of 2,4-dinitrophenol over Degussa P25 (50%) was much more significant than that of Hombikat UV-100 because of the different adsorption behavior of β -cyclodextrin over two TiO₂. Hydroxyl radical and valance band hole was found to be the predominant reactant during the degradation of 2,4-dinitrophenol using P25 and UV-100, respectively. Formic acid, acetic acid, oxalic acid, and NO₃⁻ were detected as advanced oxidation products.

Keywords: 2,4-Dinitrophenol; TiO₂; Humic acid; Cyclodextrin; Photocatalytic degradation

1. Introduction

Nitrophenol, as a kind of pesticide, is widely used in the manufacture of dyes and wood preservatives, which can easily enter the environment when it is made or used. Nowadays, nitrophenol is frequently observed in wastewater, surface water, atmosphere,

soil, and sediment samples as well as living organisms, including humans [1–6]. Because nitrophenol can cause undesired effects on organisms even when under trace level [7,8], it has been marked as a kind of first priority pollutants by many governments. Many remediation methods, such as adsorption [9], biodegradation [10], and advanced oxidation process (AOPs) [11–17], have been applied to remove nitrophenol from aqueous solutions.

*Corresponding author.

The authors Lu Mao and Jiaojun Shen made equal contribution to this work and the author order was decided by coin flipping.

Most kinds of toxic pollutants, such as organic compounds, metal ions, bacteria, and virus, can be successfully removed using TiO₂ heterogeneous photocatalysis, a typical kind of AOPs, due to the photo-generated electron-hole pair and the subsequently produced reactive oxygen species (ROS) [18–22]. The operational parameters, including aquatic pH, light intensity, photocatalyst dosage, methods of utilization of TiO₂, and temperature, were revealed to have great influence on removal efficiency of pollutants. Moreover, dissolved organic matters (DOMs) were reported to exert great effects on the degradation of pollutants, depended on operational parameters. Additionally, the size, shape, and crystalline structure of titania photocatalyst can affect the reaction pathways and photo-activity of electron-hole pair, subsequently influencing the degradation of pollutants.

The performance of two commercial TiO₂ (Degussa P25 and Hombikat UV-100) in removing 2,4-dinitrophenol (DNP) from aquatic solution was carried out under UV–visible light irradiation ($\lambda \geq 340$ nm) in this work. The primary objective is to reveal the extent to which the degradation efficiency was influenced by operational parameters (pH, dosage), properties of TiO₂ (size, crystalline, and specific surface area), and aquatic environments (DOM concentration and type). Also, photodegradation products and the mechanisms of 2,4-dinitrophenol over different TiO₂ interfaces were analyzed and discussed in this work.

2. Materials and methods

2.1. Reagents

2,4-dinitrophenol (98%) was obtained from Aladdin-Reagent Corporation (Shanghai, China) and used as a representative of nitrophenol pollutants. Hombikat UV-100 and Degussa P25, used as photocatalyst, were either directly purchased from the manufacturer or obtained from distributors. Oxalate (Sigma–Aldrich, sodium salt), humic acid (HA) (Sigma–Aldrich, sodium salt), and cyclodextrin (Aladdin-Reagent Corporation, Shanghai) were implemented as DOMs in this work. Analytical grade isopropanol (IPA), sodium azide

(NaN₃), and potassium iodine (KI) were purchased from Shanghai Reagent Co. Ltd (Shanghai, China) and used to scavenge different ROS. Deionized water (resistivity > 18.0 M Ω cm) was used during sample preparation.

2.2. Characterization of TiO₂ used in this work

The Brunauer–Emmett–Teller (BET) surface areas of the two TiO₂ were determined using a Micromeritics ASAP 2020 setup. UV–vis diffuse reflectance spectra were recorded on a Shimadzu 2550 UV–vis spectrophotometer with BaSO₄ as the background between 200 and 800 nm. The X-ray diffraction (XRD) patterns of the prepared products were recorded on a Dmax-rA powder diffractometer (Rigaku, Japan) using Cu K α radiation and a step width of $2\theta = 0.02^\circ$. Transmission electron microscopy (TEM) images were obtained on a JEOL JEM 2010HT microscope (Japan Electronics, Japan) at an accelerating voltage of 200 kV. The diameters of TiO₂ particles were determined by statistical analysis of TEM image. The physical properties of TiO₂ are listed in Table 1.

2.3. Photodegradation of 2,4-dinitrophenol (DNP) in TiO₂ dispersion

The photodegradation of DNP was performed in a self-made reactor, and a Philips Master Color lamp (CDM-T 150 W/942) whose light intensity was 266 W/m² was used as the irradiation source [23]. The emission spectrum of the lamp is given in Fig. 1. TiO₂ suspended solution containing DNP and/or DOMs was equilibrated in dark for half an hour before irradiation. Then 5 m/L aliquot was withdrawn to determine the concentration c_0 . During the whole oxidation reactions, 5 m/L aliquots were collected for each time interval, filtered, and analyzed for the concentration c_t .

The observed pseudo-first-order kinetic rate constants for degradation were obtained from a linear fit of the experimental data to Eq. (1):

$$\ln(c_0/c_t) = k_{\text{obs}} \times t + b \quad (1)$$

Table 1
Physical properties of TiO₂ used in this study

Catalysts	Crystalline form (%)		TEM diameter (nm)	BET (m ² /g)
	Anatase	Rutile		
Hombikat UV-100	100	0	5 ± 2	307
Degussa P25	71	29	25 ± 3	45

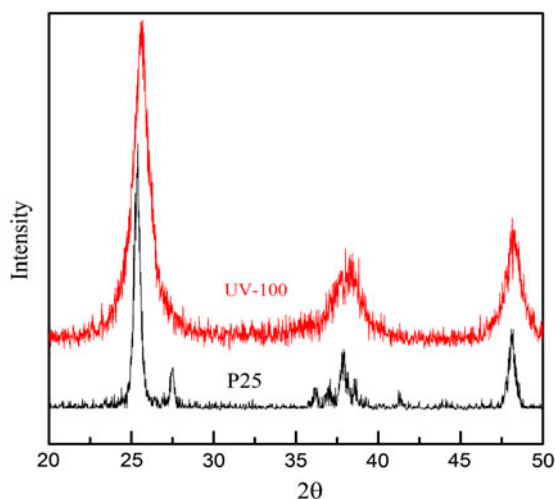


Fig. 1. XRD patterns of UV-100 and P25.

The concentrations of DNP were monitored by HPLC method. The experiments were performed using a Waters 484 HPLC with an Agilent Zorbax SB-C18 column (5 μm , 4.6 \times 150 mm). The mobile phase was a mixture of methanol and 5% acetic acid aqueous solution (70/30, v/v) with a flow rate of 1.0 m/L min⁻¹. The UV detection wavelength was set at 317 nm.

The analysis of small organic acids and inorganic ions after the degradation was performed with an ionic chromatography (ICS-9000).

All the experiments were performed in triplicate and described as the mean \pm standard deviation.

3. Results and discussion

3.1. Comparison of optical property, microstructure, crystal size, and BET surface area

As shown in Fig. 1, XRD patterns of TiO₂ show strong diffraction peaks, and all peaks are in good agreement with the standard spectrum (JCPDS No.: 88-1175 for rutile phase and 84-1286 for anatase phase). The results indicate that P25 possesses both anatase and rutile phase, while UV-100 has pure anatase phase. The calculated average grain size of P25 and UV-100 using Scherrer's equation is about 8 and 18 nm, respectively. The band gaps of rutile and anatase TiO₂ are generally consensus placed at 3.03 and 3.20 eV, respectively. Therefore, as shown in Fig. 2, P25 and UV-100 have different absorption properties. P25 has higher absorption intensity in the region from 340 to 400 nm due to the rutile phase within.

The TEM images of P25 and UV-100 is shown in Fig. 3. The results clearly show that UV-100 mainly exists in the aggregation form, while P25 exists in a

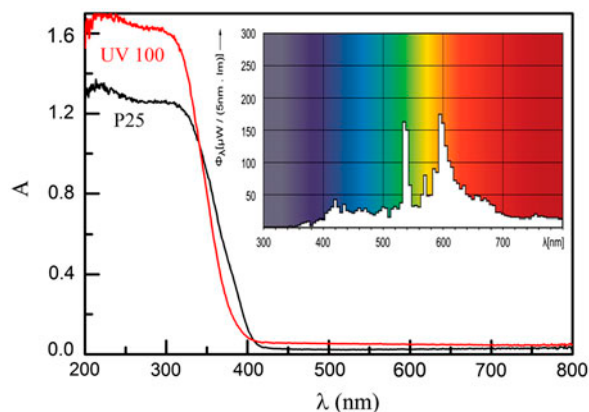


Fig. 2. UV-vis diffusion absorption spectra of P25 and UV-100, inset: emission spectra of the irradiation lamp used in this work.

more homogeneous state in the aqueous solution. The particle size for UV-100 is much smaller than P25, and the visual diameters for the two TiO₂ are close to that obtained from the Scherrer's equation. The N₂ adsorption-desorption isotherms for UV-100 and P25 are presented in Fig. 4. The BET area of UV-100 is about 307 m²/g, about 5.7 times larger than that of P25 (46 m²/g).

3.2. Effect of TiO₂ dosage on the degradation of 2,4-dinitrophenol

The photocatalytic degradation of DNP aqueous solutions with various TiO₂ concentrations is illustrated in Fig. 5. There is virtually no photolysis of DNP occurred in the absence of TiO₂ because of the lack of overlap of DNP's absorption and the emission spectrum of the lamp (Fig. 5). It is noticeable that the k_{obs} is much higher (6–12 times higher) in P25 dispersion than that in UV-100 dispersion at the same concentration of TiO₂. The photodegradation of sulfamethoxazole in P25 dispersion is also found to be much faster than that in UV-100 dispersion under UVA irradiation (324 $\leq \lambda \leq$ 400 nm) due to the low electron-hole recombination rate in irradiated P25 [24,25]. It is normally accepted that a larger specific surface area can provide more reactive sites. However, DNP has low adsorption affinity on both TiO₂ (5–12% with an initial concentration of 5 μM at different pH), making BET surface area an indistinctive factor in the photodegradation of DNP at neutral pH. Conversely, light absorption property of TiO₂ plays a major role in DNP's photodegradation. Compared with UV-100, P25 has higher absorbance from 340 to 400 nm, making P25 more efficiently irradiated. Hence, more reactive species could generate in P25 dispersion than in

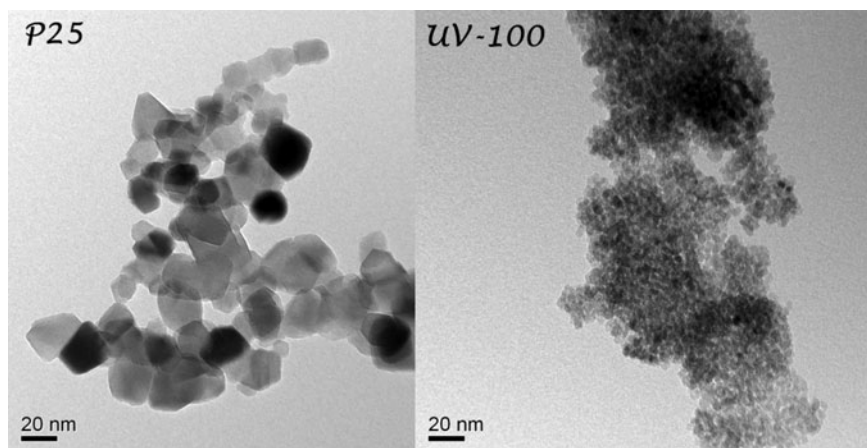


Fig. 3. TEM images of P25 and UV-100.

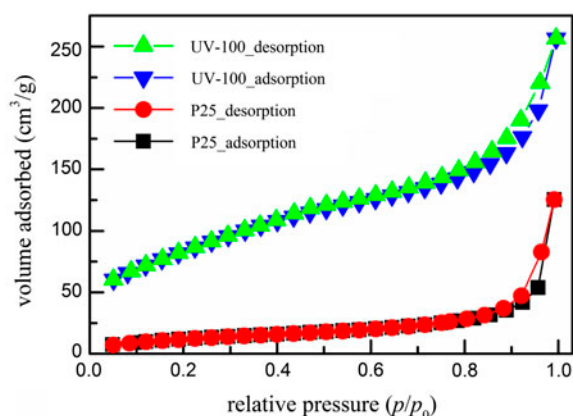


Fig. 4. N_2 adsorption–desorption isotherms over UV-100 and P25.

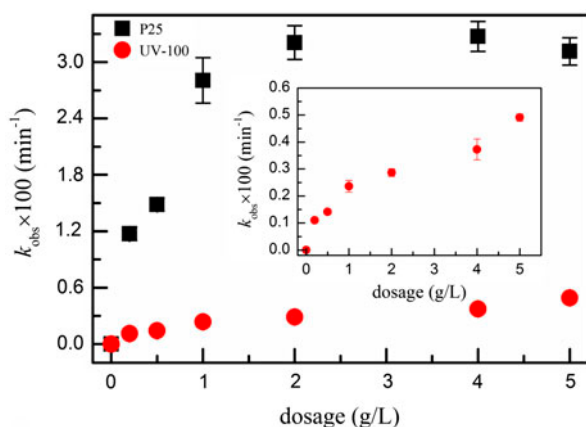


Fig. 5. Effects of TiO_2 dosage on the photodegradation kinetics of 2,4-dinitrophenol, inset: zoom out for the UV-100 section, DNP = 5 μM , pH 6.0.

UV-100 dispersion under the same irradiation condition. Moreover, it is revealed that different interfacial electron trapping behaviors play an important and unique role in the rutile/anatase morphology within Degussa P25, which is critical to the enhanced photocatalytic behavior of mixed-phase TiO_2 [25].

Apparently, in this work, the observed photodegradation kinetic constant (k_{obs}) of DNP sharply increases when the concentration of TiO_2 rises from 0.0 to 5.0 g/L using UV-100 as catalyst. This result is consistent with many studies where the reaction accelerates with the increase of TiO_2 dosage mainly because the amount of reactive species like $\cdot OH$ was dependent on the concentration of catalyst in the bulk solution. On the other side, the k_{obs} rises gradually with the increase of P25 dosage and achieves a plateau. Further increase the dosage of P25 only slightly promotes the photodegradation of DNP. The k_{obs} is 0.032 min^{-1} and 0.033 min^{-1} in 2 g/L and 4 g/L P25 dispersion, respectively. Continuously increasing the concentration of P25 results in the slight inhibition of DNP's photodegradation. The optimum amount of TiO_2 should be settled in order to avoid superfluous catalyst and also ensure total absorption of radiation photons for efficient photodegradation [20,26]. When the dose of the catalyst increases, the adsorption and degradation will be facilitated. However, high concentration of TiO_2 particles makes it much easier to aggregate and reduce the light transmission. Therefore, the concentration of TiO_2 is fixed at 2 g/L in the latter study.

3.3. Effect of solution pH on the photodegradation of 2,4-dinitrophenol

The effect of solution pH was studied in the range of 3.0–10.0 in 2 g/L TiO_2 dispersion, and the results

are demonstrated in Fig. 6. The results indicate that pH value has a significant effect on both TiO₂. The favored results for DNP photocatalytic degradation were obtained near neutral solution (i.e. pH range from 4.0 to 7.0) with a maximum at pH 6.0 in P25 dispersion whereas k_{obs} decreases sharply in the alkaline pH range. On the other side, in UV-100 dispersion, the photodegradation of DNP is much faster in acidic pH (3.0) solution and k_{obs} has no obvious change from pH 4.0 to pH 10.0.

It is well known that interpreting the effects of pH on the photodegradation of organic pollutants is a very difficult process, which is generally related to multiple factors such as electrostatic interactions among the semiconductor surface, solvent molecules, substrate, and charged radicals formed during the reaction process. The favored pH for the photodegradation of DNP in P25 dispersion is nearby the point of zero charge (pzc) of P25 (pH 6.8, Fig. 7). The best pH for the degradation of 4-nitrophenol in P25 dispersion is also found to be near the pzc [27]. That probably indicates that the influence of pH on the degradation of DNP results from the effect of pH on P25 itself. Hydroxyl radicals are considered as the predominant species at neutral or high pH levels [26]. Although it is suggested that $\cdot\text{OH}$ is easier to be formed by oxidizing more hydroxide ions available on TiO₂ surface in alkaline solution [26,28], it should be noted that there is a Coulombic repulsion between the negative charged surface of photocatalyst and the hydroxide anions as well as the repulsion between the negative charged surface and the negative form of DNP, which could prevent the formation of $\cdot\text{OH}$ and thus decrease the photodegradation of DNP at high pH.

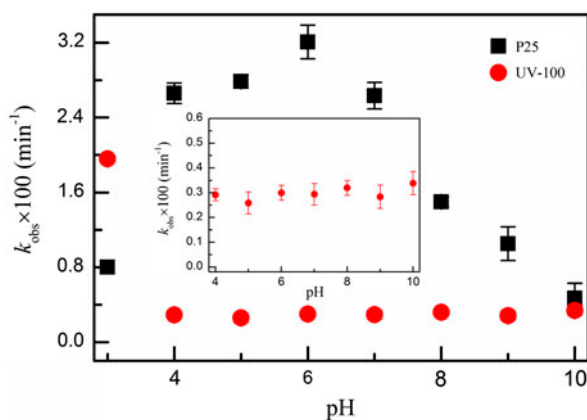


Fig. 6. Effects of pH on the photodegradation kinetics of 2,4-dinitrophenol, inset: zoom out for the UV-100 section, TiO₂ = 2 g/L, DNP = 5 μM .

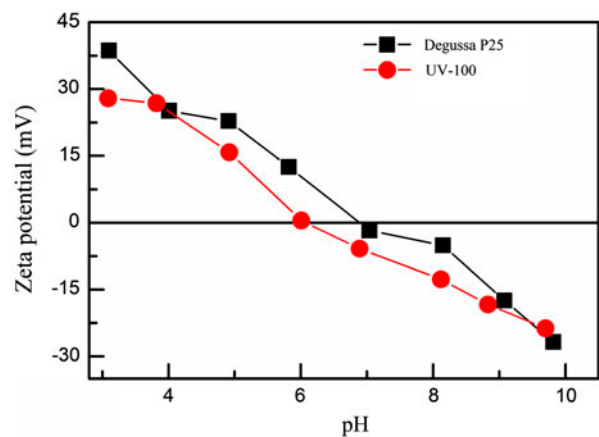


Fig. 7. Zeta potential of TiO₂ as a function of pH.

It is noted that the effect of pH on the photodegradation of DNP in UV-100 dispersion is highly different from that in P25. The degradation of DNP is only faster in UV-100 than that in P25 at pH 3.0. The positive holes are regarded as the major oxidation species at low pH [26]. Hence, UV-100 could provide more chances for the reaction between surface-trapped holes and DNP than P25 because of its much larger BET surface areas. Moreover, TiO₂ particles tend to agglomerate under acidic condition and the surface area available for DNP adsorption and photon absorption would be reduced, which suggests BET area plays a vital role in the photodegradation of DNP at low pH.

3.4. Effect of HA on the photodegradation of 2,4-dinitrophenol

HA is often considered to be the most common water constituent that affects the photocatalytic degradation of target pollutants because of its multiple functions interfering the adsorption of target pollutants to catalyst surface, competing for the adsorption of photons, inducing photosensitized degradation, and removing ROS [24,29,30]. The photodegradation of DNP under different HA concentration is presented in Fig. 8. As can be seen, HA significantly suppresses the photodegradation of DNP in both P25 and UV-100 dispersion in a range from 0 to 20 mg/L. The results indicate that the reaction of DNP with reactive species generated by HA is insignificant, compared with the increasing scavenging of the reactive species by HA itself. At high concentration of HA, inner filter effects and light scattering by HA also make a contribution to the inhibition of DNP photodegradation.

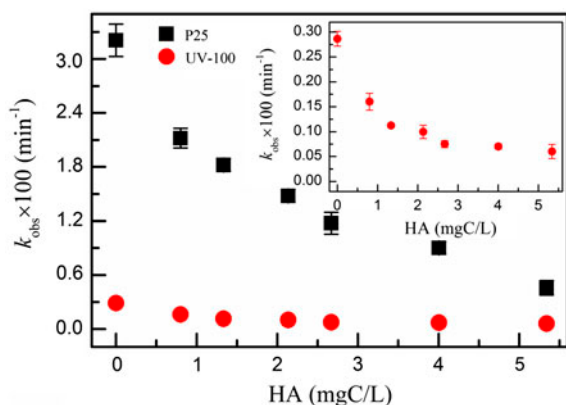


Fig. 8. Effects of HA concentration on the photodegradation kinetics of 2,4-dinitrophenol, inset: zoom out for the UV-100 section, $TiO_2 = 2$ g/L, DNP = 5 μ M, pH 6.0.

3.5. Effect of β -CD on the photodegradation of 2,4-dinitrophenol

Although β -CD is not the common constituent in environmental water samples, it is widely used in soil remediation by means of soil flushing. Therefore, β -CD has become a major co-exist compound with the target pollutants. The effects of β -CD on the photodegradation of DNP were also investigated in this work. As shown in Fig. 9, the photodegradation of DNP is retarded in the presence of 5 μ M β -CD. In 5 μ M β -CD solution, k_{obs} is 0.52 and 0.90 times of that observed in the absence of β -CD over P25 and UV-100, respectively. Compared with the effect of 5 μ M β -CD, further increase of β -CD to 20 μ M has no obvious different effects on the photodegradation of DNP. The negative effects of β -CD on the photodegradation of DNP are different from its positive influences on the photodegradation of other pollutants such as bisphenol A, 4,4'-biphenol, and dye pollutants probably because of low inclusion complex ability between DNP and β -CD or unflavored inclusion pattern.

The discrepancy of suppression extent probably results from the different adsorption affinity of β -CD over the two TiO_2 . The adsorption onto UV-100 is much greater than that onto P25 because UV-100 possesses a larger BET surface area. Therefore, the bulk concentration of β -CD in P25 dispersion is larger than that in UV-100 dispersion retarding the diffusion onto TiO_2 more efficiently and slowing down the degradation of DNP subsequently.

3.6. Preliminary mechanism for the degradation of 2,4-dinitrophenol

The activity of TiO_2 was derived from the photogenerated electron-hole pair and the following

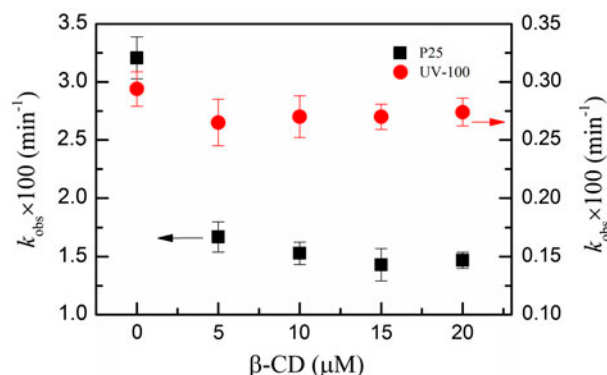


Fig. 9. Photodegradation of 10 μ M 2,4,6-trichlorophenol in 2 g/L magnetic TiO_2 dispersion, $TiO_2 = 2$ g/L, DIP = 5 μ M, pH 6.0.

reactions. $O_2^{\cdot-}/HO_2^{\cdot}$, H_2O_2 , $\cdot OH$, and 1O_2 could make a contribution to the degradation of pollutants by TiO_2 photocatalysis. Different radical quenchers were added to the TiO_2 dispersion, respectively, to identify the predominant radicals and analyze the possible transformation channels of DNP by TiO_2 photocatalysis. Iodide added to the solution would scavenge the generated holes (h_{vb}^+) and its surface would adsorb hydroxyl radical ($\cdot OH_s$) [31]. As shown in Fig. 10, the degradation of DNP is significantly suppressed in the presence of 10 mM KI, which indicates that both h_{vb}^+ and $\cdot OH_s$ together are responsible for the major degradation of DNP by P25 photocatalysis. Further degradation of DNP in the presence of 56 mM IPA, aiming to distinguish the relative contribution of h_{vb}^+ and $\cdot OH_s$ to the degradation of DNP, shows that the degradation of DNP was also highly retarded in the presence of IPA due to its competition for $\cdot OH$, which means that $\cdot OH$ is the predominant reactant whereas direct hole oxidation is a minor channel during the degradation of DNP.

The presence of 10 mM KI also decelerates the degradation of DNP using UV-100. However, the existence of IPA highly accelerates the degradation in the opening 30 min. Subsequently, the degradation exists a slow phase (circle plot). The degradation could be accelerated in the presence of extra 56 mM IPA after 30 min reactions (arrow point in the diamond plot). The results indicated $\cdot OH$ alone makes barely contribution to the degradation of DNP. In the presence of both IPA and KI, the degradation of DNP followed the same trends as the degradation in the presence of KI alone. These results indicate direct hole oxidation is the main path for the degradation of DNP by UV-100 photocatalysis. The enhanced influence of IPA is probably from the low electron-hole recombination rate because of the quench of $\cdot OH$.

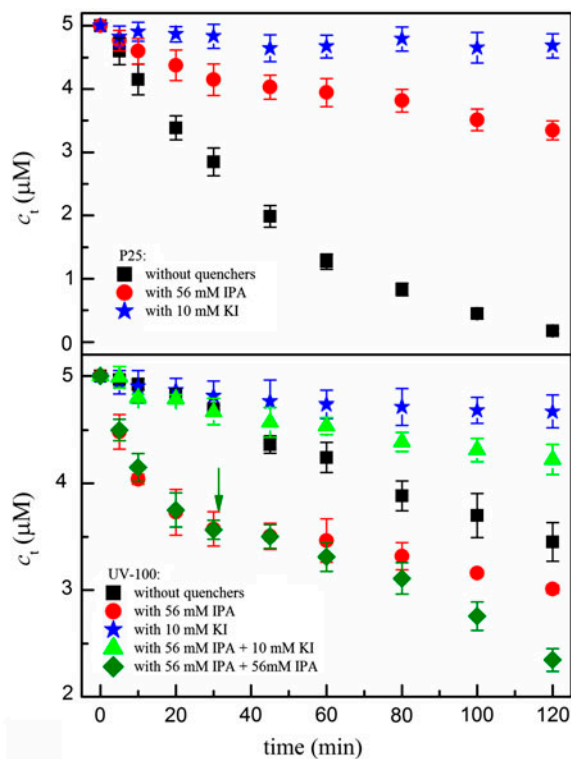


Fig. 10. Effects of radical scavengers on the degradation of DNP by Degussa P25 (upper panel) and UV-100 (lower panel). The arrow point the addition of another 56 mM IPA to diamond plot.

The oxidation of DNP by $\cdot\text{OH}$ and valence band hole could induce hydroxylation or the release of NO_2^- during the degradation of 4-nitrophenol [32]. Analogous degradation paths were expected for the degradation of DNP by TiO_2 photocatalysis. Subsequently, further oxidation of early aromatic intermediates could result in the breakdown of their aromatic structures. In this work, formic acid, acetic acid, oxalic acid, and NO_3^- were detected as advanced oxidation products of DNP both by Degussa P25 and Hombikat UV-100 after 4 h irradiation.

4. Conclusions

The results indicate that the photodegradation of 2,4-dinitrophenol, very different in two commercial TiO_2 , depends on the catalyst loading, solution pH, dissolved HA, and β -cyclodextrin. Although Hombikat UV-100 possesses a much larger specific surface area, the observed kinetics (k_{obs}) in P25 for the photodegradation of 2,4-dinitrophenol was 6–12 times higher than that in Hombikat UV-100. The favored results for 2,4-dinitrophenol photocatalytic degradation is obtained at

near neutral solution in P25 dispersion, and k_{obs} decreases sharply in the alkaline pH range. As for the photodegradation of 2,4-dinitrophenol in UV-100 dispersion, k_{obs} is much larger at acidic pH (3.0) than that of other solution pH values. Dissolved HA shows significant negative effects on the photodegradation of 2,4-dinitrophenol. In the presence of 20 mg/L HA, k_{obs} is found to be only 15% (Degussa P25) and 21% (Hombikat UV-100) of the values obtained from the corresponding pure aquatic solutions. β -Cyclodextrin suppresses the photodegradation of 2,4-dinitrophenol to different extents over Degussa P25 and Hombikat UV-100 because of its different adsorption affinity over two TiO_2 . Carboxylic acids and inorganic nitrate were detected as the final degradation products, which indicate that TiO_2 photocatalysis is an effective method to remove 2,4-dinitrophenol from wastewater without producing any other final products with higher toxicity.

Acknowledgment

This work has been supported by National Science Foundation for Fostering Talents in Basic Research (No. J1103409), Undergraduate Science Research Project of Wuhan University (No. 1310486035), the National Natural Science Foundation of China (No. 21207104), and the Youth Chenguang Project of Science and Technology of Wuhan City (No. 2013070104010009). We thank the Large-scale Instrument and Equipment Sharing Foundation of Wuhan University.

References

- [1] M.A.J. Harrison, S. Barra, D. Borghesi, D. Vione, C. Arsene, R. Iulian Olariu, Nitrated phenols in the atmosphere: A review, *Atmos. Environ.* 39 (2005) 231–248.
- [2] C. Ye, Q. Zhou, X. Wang, J. Xiao, Determination of phenols in environmental water samples by ionic liquid-based headspace liquid-phase microextraction coupled with high-performance liquid chromatography, *J. Sep. Sci.* 30 (2007) 42–47.
- [3] J. Jin, C. Wang, Y. Tao, Y. Tan, D. Yang, Y. Gu, H. Deng, Y. Bai, H. Lu, Y. Wan, Z. Lu, Y. Li, Determination of 3-nitrotyrosine in human urine samples by surface plasmon resonance immunoassay, *Sens. Actuators, B* 153 (2011) 164–169.
- [4] P. Bastos, P. Haglund, The use of comprehensive two-dimensional gas chromatography and structure-activity modeling for screening and preliminary risk assessment of organic contaminants in soil, sediment, and surface water, *J. Soils Sediments* 12 (2012) 1079–1088.
- [5] C. Hu, B. Chen, M. He, B. Hu, Amino modified multi-walled carbon nanotubes/polydimethylsiloxane coated stir bar sorptive extraction coupled to high performance liquid chromatography-ultraviolet detection for the determination of phenols in environmental samples, *J. Chromatogr. A* 1300 (2013) 165–172.

- [6] M. Khairy, Assessment of priority phenolic compounds in sediments from an extremely polluted coastal wetland (Lake Maryut, Egypt), *Environ. Monit. Assess.* 185 (2013) 441–455.
- [7] C. Liu, D. Yong, D. Yu, S. Dong, Cell-based biosensor for measurement of phenol and nitrophenols toxicity, *Talanta* 84 (2011) 766–770.
- [8] D.T. Sponza, Ö.S. Kuscü, Relationships between acute toxicities of para nitrophenol (p-NP) and nitrobenzene (NB) to *Daphnia magna* and *Photobacterium phosphoreum*: Physicochemical properties and metabolites under anaerobic/aerobic sequential, *J. Hazard. Mater.* 185 (2011) 1187–1197.
- [9] G. Xue, M. Gao, Z. Gu, Z. Luo, Z. Hu, The removal of p-nitrophenol from aqueous solutions by adsorption using gemini surfactants modified montmorillonites, *Chem. Eng. J.* 218 (2013) 223–231.
- [10] M.C. Tomei, M.C. Annesini, S. Bussoletti, 4-nitrophenol biodegradation in a sequencing batch reactor: Kinetic study and effect of filling time, *Water Res.* 38 (2004) 375–384.
- [11] K.H. Wang, Y.H. Hsieh, M.Y. Chou, C.Y. Chang, Photocatalytic degradation of 2-chloro and 2-nitrophenol by titanium dioxide suspensions in aqueous solution, *Appl. Catal., B* 21 (1999) 1–8.
- [12] M.A. Oturan, J. Peiroten, P. Chartrin, A.J. Acher, Complete destruction of p-nitrophenol in aqueous medium by electro-Fenton method, *Environ. Sci. Technol.* 34 (2000) 3474–3479.
- [13] A. Goi, M. Trapido, Hydrogen peroxide photolysis, Fenton reagent and photo-Fenton for the degradation of nitrophenols: A comparative study, *Chemosphere* 46 (2002) 913–922.
- [14] A. Di Paola, V. Augugliaro, L. Palmisano, G. Pantaleo, E. Savinov, Heterogeneous photocatalytic degradation of nitrophenols, *J. Photochem. Photobiol., A* 155 (2003) 207–214.
- [15] L. Tao, F. Li, C. Feng, K. Sun, Reductive transformation of 2-nitrophenol by Fe(II) species in γ -aluminum oxide suspension, *Appl. Clay Sci.* 46 (2009) 95–101.
- [16] M.V. Bagal, B.J. Lele, P.R. Gogate, Removal of 2,4-dinitrophenol using hybrid methods based on ultrasound at an operating capacity of 7L, *Ultrason. Sonochem.* 20 (2013) 1217–1225.
- [17] Z. Zhu, L. Tao, F. Li, Effects of dissolved organic matter on adsorbed Fe(II) reactivity for the reduction of 2-nitrophenol in TiO₂ suspensions, *Chemosphere* 93 (2013) 29–34.
- [18] M.R. Hoffmann, S.T. Martin, W. Choi, D.W. Bahnemann, Environmental applications of semiconductor photocatalysis, *Chem. Rev.* 95 (1995) 69–96.
- [19] A. Fujishima, T.N. Rao, D.A. Tryk, Titanium dioxide photocatalysis, *J. Photochem. Photobiol., C* 1 (2000) 1–21.
- [20] U.I. Gaya, A.H. Abdullah, Heterogeneous photocatalytic degradation of organic contaminants over titanium dioxide: A review of fundamentals, progress and problems, *J. Photochem. Photobiol., C* 9 (2008) 1–12.
- [21] J.H. Mo, Y.P. Zhang, Q.J. Xu, J.J. Lamson, R.Y. Zhao, Photocatalytic purification of volatile organic compounds in indoor air: A literature review, *Atmos. Environ.* 43 (2009) 2229–2246.
- [22] A. Markowska-Szczupak, K. Ulfig, A.W. Morawski, The application of titanium dioxide for deactivation of bioparticulates: An overview, *Catal. Today* 169 (2011) 249–257.
- [23] X. Zhang, F. Wu, N. Deng, Efficient photodegradation of dyes using light-induced self assembly TiO₂/ β -cyclodextrin hybrid nanoparticles under visible light irradiation, *J. Hazard. Mater.* 185 (2011) 117–123.
- [24] L. Hu, P.M. Flanders, P.L. Miller, T.J. Strathmann, Oxidation of sulfamethoxazole and related antimicrobial agents by TiO₂ photocatalysis, *Water Res.* 41 (2007) 2612–2626.
- [25] D.C. Hurum, K.A. Gray, T. Rajh, M.C. Thurnauer, Recombination pathways in the Degussa P25 formulation of TiO₂: Surface versus lattice mechanisms, *J. Phys. Chem. B* 109 (2004) 977–980.
- [26] M.H. Habibi, A. Hassanzadeh, S. Mahdavi, The effect of operational parameters on the photocatalytic degradation of three textile azo dyes in aqueous TiO₂ suspensions, *J. Photochem. Photobiol., A* 172 (2005) 89–96.
- [27] D. Chen, A.K. Ray, Photodegradation kinetics of 4-nitrophenol in TiO₂ suspension, *Water Res.* 32 (1998) 3223–3234.
- [28] A. Fujishima, X. Zhang, D.A. Tryk, TiO₂ photocatalysis and related surface phenomena, *Surf. Sci. Rep.* 63 (2008) 515–582.
- [29] X. Zhao, X. Quan, H. Zhao, S. Chen, Y. Zhao, J. Chen, Different effects of humic substances on photodegradation of p, p'-DDT on soil surfaces in the presence of TiO₂ under UV and visible light, *J. Photochem. Photobiol., A* 167 (2004) 177–183.
- [30] E. Selli, D. Baglio, L. Montanarella, G. Bidoglio, Role of humic acids in the TiO₂-photocatalyzed degradation of tetrachloroethene in water, *Water Res.* 33 (1999) 1827–1836.
- [31] S.T. Martin, A.T. Lee, M.R. Hoffmann, Chemical mechanism of inorganic oxidants in the TiO₂/UV process: Increased rates of degradation of chlorinated hydrocarbons, *Environ. Sci. Technol.* 29 (1995) 2567–2573.
- [32] W. Zhang, X. Xiao, T. An, Z. Song, J. Fu, G. Sheng, M. Cui, Kinetics, degradation pathway and reaction mechanism of advanced oxidation of 4-nitrophenol in water by a UV/H₂O₂ process, *J. Chem. Technol. Biotechnol.* 78 (2003) 788–794.